

Numerical Simulation of Performance and Exhaust Emissions of a Marine Main Engine Using Heavy Fuel Oil during the whole Voyage

Thuy Chu Van^{1,2}, Huong Nguyen Lan², Nho Luong Cong², Vikram Garaniya³, Sanaz Jahangiri³, Rouzbeh Abbassi³, Rong Situ⁴, Michael D. Ferraris⁴, Richard Kimball⁵, Zoran Ristovski¹, Thomas Rainey¹, Ali Mohammad Pourkhesalian¹, Richard J. Brown¹

¹Queensland University of Technology

2 George St, Brisbane City, Queensland, 4000, Australia

²Vietnam Maritime University

484 Lach Tray street, district Le Chan, Hai Phong, Vietnam.

³Australian Maritime College

100 Newnham Dr, Newnham, Tasmania, 7248, Australia

⁴James Cook University

1 James Cook Dr, Townsville City, Queensland, 4811, Australia

⁵Maine Maritime Academy

1 Pleasant St, Castine, Maine, 04420, USA

Abstract

In this study, the performance and exhaust emissions of the marine main engine (ME) of a large cargo vessel operating on the east coast of Australia by numerical thermodynamic simulation were investigated. The simulation were validated using on-board measurements of the ME conducted in October and November 2015 on a large cargo ship cruising between Ports of Brisbane, Gladstone and Newcastle. The commercial engine modelling/design software, AVL Boost, was used with special adaptation to marine engines and Heavy Fuel Oil (HFO). All measurements here carried out on the ME at different engine speeds and loads when the ship experienced different working conditions such as manoeuvring near port areas and cruising at sea. Specific engine parameters including in-cylinder mean and peak pressure, power, exhaust temperature and turbocharger boost were investigated. A good agreement between experimental and numerical results was observed for engine emissions of NO_x and soot at higher engine speed conditions. The capacity of AVL Boost for marine engine simulation is evaluated, including prediction on the engine performance and emissions under different engine working conditions where they cannot be measured in the experiment.

Keywords: *Exhaust emissions, AVL Boost, Heavy Fuel Oil, performance*

1. INTRODUCTION

Shipping is considered one of the most fuel efficient means of transportation [1], it accounts for over 90% of world trade by some 90,000 marine vessels [2]. However, exhaust emissions from ships have a negative impact on environment and consequently on human health [3]-[10] and

have become of global concern over the last decade [11]. To make the matters worse, these ships also burn low quality Heavy Fuel Oil (HFO) owing to its economic benefit [5]. HFO is the main fuel for around 95% of 2-stroke low-speed large-power marine main engine and approximately 70% of 4-stroke medium-speed engines [1]. HFO combustion results in different

compounds like sulphates, organic carbon (OC), black carbon (BC), ash and heavy metals in emitted particles [3],[7],[12], most which result in high toxicity risks [6]. In particular, shipping-related fine particle (PM_{2.5}) emissions alone can account for nearly 60,000 cardiopulmonary and lung cancer deaths each year [10]. Quantitative and qualitative research on ship emissions are needed for a deeper understanding for law makers and regulators [1], and becoming more important [8].

Based on a review of the literature related to ship emissions, on-board measurement studies are essential to investigate realistic emission factors, but a very limited number of such studies have been undertaken [8],[13]. This may be due to ship emission measurements being an extremely complex task that needs the participation of a wide range of collaborators and modern instrumentations. An alternative way for ship emission research has been undertaken recently by using numerical simulation tools such as AVL Boost. Boost is able to simulate a wide variety of engines including 4-stroke, 2-stroke, spark or auto-ignited types, ranging from small capacity engines up to large engines for marine engines [14]. However, in the existing literature, there are a limited number of simulation studies on marine large-power engines [15],[16].

This paper will develop an approach for HFO to be modelled using AVL Boost, and investigate the engine performance and emissions from a two-stroke, low-speed, large-output marine main engine using HFO at different engine load conditions. Results are validated against experimental data collected from on-board ship emission measurements campaign.

2. ON-BOARD SHIP EMISSION MEASUREMENT CAMPAIGN AND NUMERICAL SIMULATION

2.1. Ship emission measurement campaign

The measurements were performed in October and November 2015 on two large cargo ships (called Vessel I and Vessel II) at Port of Brisbane, Gladstone, and Newcastle. The work was a collaboration of the Australian Maritime College (AMC), Queensland University of Technology (QUT), and the Maine Maritime Academy (MMA) and funded by the International Association of Maritime Universities (IAMU). The first on-board measurement was performed on Vessel I from 26th to 31st of October, 2015 when she was sailing from Port of Brisbane to Port of Gladstone. The second measurement was conducted on Vessel II from 03th to 06th of November, 2015 in her passage from Gladstone to Newcastle. All measurements have been carried out on both main and auxiliary engines of the two ships for different operating ship conditions, experienced at berth, manoeuvring, and at sea. The on-board measurement values presented in this paper for validating numerical simulation were from the main engine of Vessel II. The detail of on-board ship emission measurement results, the experimental methodology, and instrumentation can be found in the previous study [14].

2.2. Numerical simulation

2.2.1. Theory of AVL Boost

The first law of thermodynamics applied to the combustion chamber is that the change of the internal energy in the cylinder is equal to the sum of piston work, fuel heat input, wall heat losses and the enthalpy flow due to blow-by. This is applied in AVL Boost to calculate the thermodynamic state of the cylinder [15].

$$\frac{d(m_c \cdot u)}{d\alpha} = -p_c \cdot \frac{dV}{d\alpha} + \frac{dQ_F}{d\alpha} - \sum \frac{dQ_W}{d\alpha} - h_{BB} \cdot \frac{dm_{BB}}{d\alpha} \quad (1)$$

where m_c : mass in the cylinder; u : specific internal energy; p_c : cylinder pressure; V : cylinder volume; Q_F : fuel energy; Q_W : wall

heat loss; α : crank angle; h_{BB} : enthalpy of blow-by; m_{BB} : blow-by mass flows.

The heat transfer to the walls of the combustion chamber including cylinder head, piston, and cylinder liner can be calculated as follow [15].

$$Q_{wi} = A_i \cdot \alpha_i \cdot (T_c - T_{wi}), \quad (2)$$

where Q_{wi} : wall heat flow (cylinder head, piston, cylinder liner); A_i : surface area (cylinder head, piston, cylinder liner); α_i : heat transfer coefficient; T_c : gas temperature in the cylinder; T_{wi} : wall temperature (cylinder head, piston, cylinder liner).

In order to calculate the heat transfer coefficient α_i , Woschni 1978 heat transfer model was used in this paper, and presented as follow:

$$\alpha_i = \frac{1.13 \cdot p_{c,0}^{0.75} \cdot T_{c,1}^{0.75} \cdot V_D^{0.25} \cdot c_m}{D \cdot \left(1 + 1.5 \cdot \frac{V_D}{D} \right)} \quad (3)$$

where $C_1 = 2.28 + 0.308 \cdot c_u/c_m$; $C_2 = 0.00324$ for DI engines; D : cylinder bore; c_m : mean piston speed; c_u : circumferential velocity; V_D : displacement per cylinder; $p_{c,0}$: cylinder pressure of the motored engine (bar); $T_{c,1}$: temperature in the cylinder at intake valve closing (IVC); $p_{c,1}$: pressure in the cylinder at IVC (bar).

The combustion in the direct injection compression ignition engines can be considered by two processes including premixed combustion (PMC) and mixing controlled combustion (MCC) [15].

$$\dot{Q}_{total} = \dot{Q}_{PMC} + \dot{Q}_{MCC} \quad (4)$$

where Q_{total} : total heat release over the combustion process [kJ]; Q_{PMC} : total fuel heat input for the premixed combustion [kJ]; Q_{MCC} : cumulative heat release for the mixture controlled combustion [kJ].

Premixed combustion model:

A Vibe function is used to describe the actual heat release due to the premixed combustion [15].

$$\dot{Q}_{PMC} = \frac{m_{fuel, id} \cdot C_{PMC}}{\Delta \alpha_c} \cdot \left(\frac{U}{a} \right)^m \cdot \left(\frac{L}{a} \right)^a \quad (5)$$

where Q_{PMC} : total fuel heat input for the premixed combustion ($Q_{PMC} = m_{fuel, id} \cdot C_{PMC}$); $m_{fuel, id}$: total amount of fuel injected during the ignition delay phase; C_{PMC} : premixed combustion parameter; $\Delta \alpha_c$: premixed combustion duration ($\Delta \alpha_c = \frac{2\pi}{360} \cdot C_{PMC_Dur}$); C_{PMC_Dur} : premixed combustion duration factor; m : shape parameter; a : Vibe parameter.

NO_x formation model is based on the well-known Zeldovich mechanism with 6 reactions introduced in Table 1 [15].

Table 1 NO_x formation reactions

	Stoichiometry	Rate
R ₁	$N_2 + O = NO + N$	$r_1 = k_1 \cdot C_{N_2} \cdot C_O$
R ₂	$O_2 + N = NO + O$	$r_2 = k_2 \cdot C_{O_2} \cdot C_N$
R ₃	$N + OH = NO + H$	$r_3 = k_3 \cdot C_{OH} \cdot C_N$
R ₄	$N_2O + O = NO + N$	$r_4 = k_4 \cdot C_{N_2O} \cdot C_O$
R ₅	$O_2 + N_2 = N_2O + O$	$r_5 = k_5 \cdot C_{O_2} \cdot C_{N_2}$
R ₆	$OH + N_2 = N_2O + H$	$r_6 = k_6 \cdot C_{OH} \cdot C_N$

Soot formation is described by two steps including formation and oxidation. The net rate of change in soot mass m_{soot} is the difference between the rates of soot formed $m_{soot,form}$ and oxidized $m_{soot,ox}$ [14].

$$\frac{dm_{soot}}{dt} = m_{soot,form} - m_{soot,ox} \quad (7)$$

2.2.2. HFO setup in AVL Boost

In order to bring the convenience for users, AVL Boost offers fuel species with their thermodynamic properties in an internal database. In particular, fuels such as diesel, ethanol, methanol, methane are available for fuel properties. Although HFO is not defined and consequently not available in the fuel list, using AVL Boost Gas Properties tool can help solve this obstacle.

In principal, all species that are defined in the species list can be a component of the fuel as presented in Fig. 1.

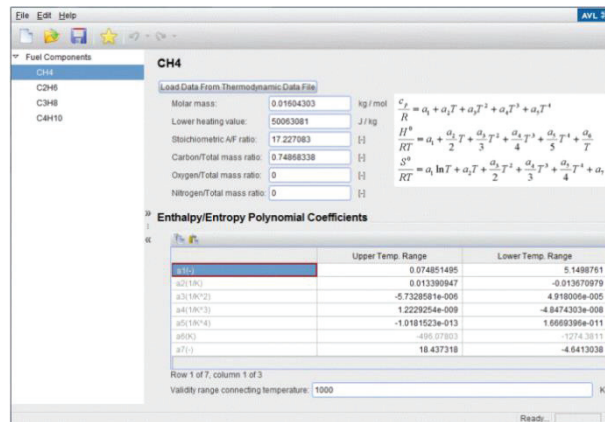


Fig. 1 Fuel component set-up

The individual fuel component fraction ratios can be specified by mass or volume of this component relative to the total fuel mass or volume. The entire table of Enthalpy/Entropy Polynomial Coefficients for two temperature ranges are based on NASA Polynomials.

2.2.3. Marine main engine model

The modelled engine is a 2-stroke low-speed large-output marine main diesel engine used on a large bulk carrier using HFO. This engine was built in 2002 and complies with IMO Tier 1 standard for NO_x regulation. The specifications of the engine are presented in Table 2. According to the engine structure and specifications, 1 1-D working process simulation model that is illustrated in Figure 2, was created by using AVL Boost v2014.1.

Table 2 Technical parameters of the main engine

Parameter	Value
Name	Man B&W 6S50MC
Number of cylinders	6

Bore x stroke (mm)	500 x 1910
Output (kW)	6,880
Rated speed (RPM)	102
BMEP (MPa)	1.8
Fire order	1-5-3-4-2-6
Build year	2002

In Fig. 2, SB1 and SB2 are the inlet and outlet boundaries; TC1 is the turbine and compressor (charger) respectively; CO1 is the turbo-charged air cooler; C1 though C6 represent six cylinders of the engine; VP1 though VP6 represent the scavenging ports (intake ports); PL1 is a scavenging air receiver; PL2 is an exhaust gas manifold and MP1 though MP8 are measurement points.

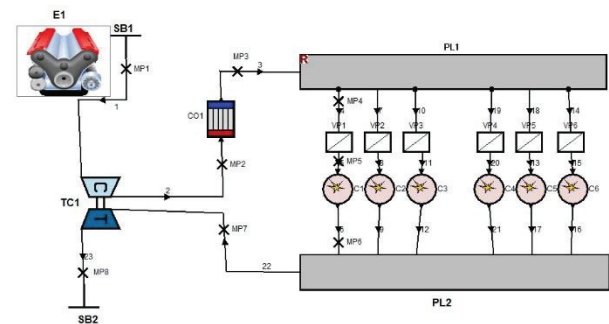


Fig. 2 One-dimensional (1-D) model of the marine main engine

3. Results and discussion

The model was validated by means of comparison between simulation results and measurement values as presented in Figure 3. The measured values were obtained as the main engine was running at 93.3 RPM and 5426.8 kW load (around 78.8% maximum continuous rate (MCR)), while the ship was at sea. A reasonable agreement between experimental and numerical values is found and presented in Fig. 3.

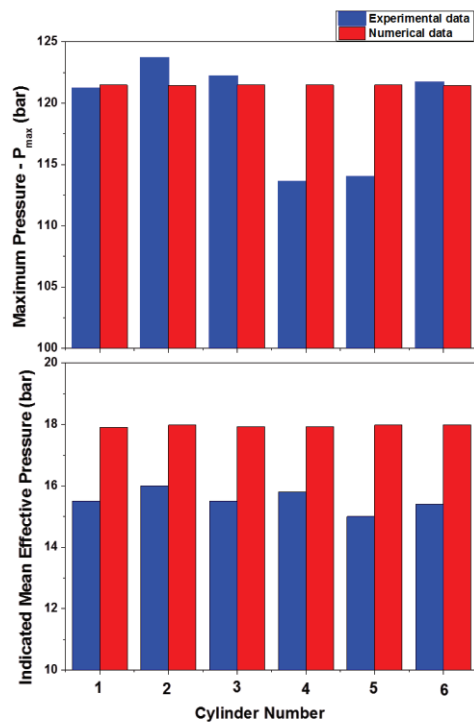


Fig. 3 Comparison of experimental and numerical values for maximum and indicated mean effective pressure for cylinders for the engine running at 93.3 RPM and 5426.8 kW load

The average deviation is around 1.7% for the maximum pressure. Measured maximum pressure for cylinders 4 and 5 are significantly lower most likely indicating the need for adjustment of the unit injectors on these cylinders. The variation between these cylinders and those at a higher pressure is within the normal operating limits of low speed marine diesel engines. Variation in the numerical maximum pressures for cylinders 1 through 6 is found in Figure 3 and caused by pressure variations in the inlet manifold which are modelled as 1 dimensional pipe flow using the Euler equation. The average deviation for IMEP is nearly 13.5%. This is most likely due to non-realistic engine parameters in the configuration file for the numerical model. Inlet and exhaust port configurations and wall roughnesses had to be estimated in the model and may not be completely realistic. Given that marine main diesel engine directly drives the

propeller shaft and propeller, thus the engine is working at speed characteristics. On-board measurements were carried out at different engine speeds, so the AVL model was also tested with a wide range of speed modes.

A comparison of experimental and numerical engine performance results is presented in Fig. 4. The general shape of both the experimental measurements and numerical results are similar. There is a greater deviation at 65 RPM from the power curve. The reason is not clearly understood, but given the data was taken on an actual ship at sea, conditions such as sea state, current wind and heading could significantly affect the power and could explain this anomaly.

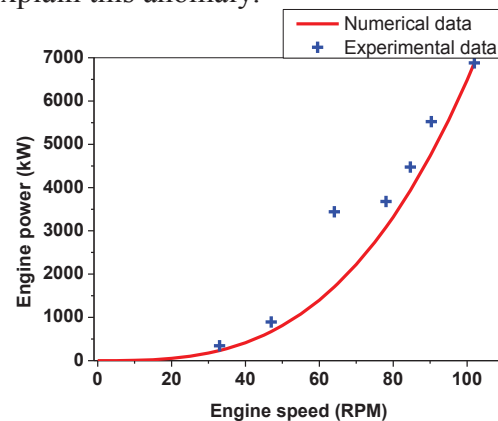


Fig. 4 Comparison between experimental and numerical values of engine power at its different speeds

Figure 5 shows a comparison between the measured and predicted NO_x emissions for the marine main engine fuelled HFO, running at different engine speeds. Emission factors of NO_x observed in Figure 5 satisfy the NO_x requirements of IMO Tier I for all cases. Owing to engine safety reason, NO_x emission factor at the maximum engine speed was not obtained, but it can be predicted by using AVL Boost simulation.

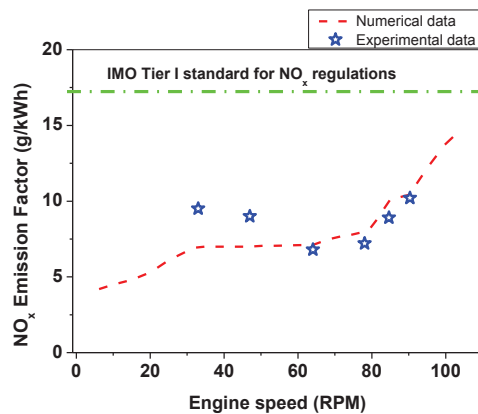


Fig. 5 Comparison for NO_x emissions with the engine running at different speeds; all cases comply with the NO_x limit of IMO Tier I regulations

Finally, soot emissions for both measurement and simulation at the different engine speeds are shown in Fig. 6. At higher engine speeds the agreement is good. At low speeds around 15% difference was observed. Soot emissions in on-board measurements were higher than that of simulation results at all engine speed modes. The simple modelling assumptions for predicting soot are clearly working well in this case.

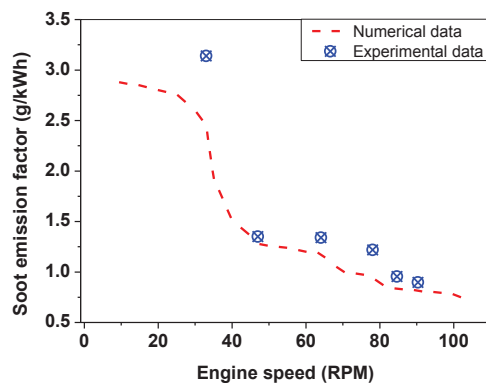


Fig. 6 Comparison for soot emissions with the engine running at different speeds

4. Conclusions

In this paper, a 2-stroke low-speed large-power main engine installed in a large bulk carrier was numerically modelled by using the first law of thermodynamics-based AVL Boost tool in order to obtain and predict engine performance and emissions.

HFO was characterized, and then set-up into the simulation. Results were validated against on-board ship emission measurement campaign data with reasonable agreement for engine parameters and good agreement for emission parameters. Through this application, AVL Boost can offer prediction of engine performance and emissions under a wide range of engine working conditions in which the experimental measurements cannot be obtained such as at the maximum engine load or engine speed.

5. Acknowledgments

The authors gratefully acknowledge the Port of Brisbane Corporation for their ongoing support in the project, Maritime Safety Queensland and stevedore operators (AAT, Patricks and DP World). The authors would like to acknowledge the outstanding support received from all employees and crew of CSL Group Inc. A special thanks to Ms Rhiannah Carver and Mr Jovito Barrozo from CSL Australia for their assistance in coordinating this project. In addition, the materials and data in this publication have been obtained through the support of the International Association of Maritime Universities (IAMU) and the Nippon Foundation in Japan. Lastly, the help provided by Miran Vogrinc, an AVL staff is also highly appreciated.

References

- [1] J.J. Corbett. Updated emissions from ocean shipping 108 (D20) (2003) 4650-4665.
- [2] V. Eyring. Emissions from international shipping: 2. Impact of future technologies on scenarios until 2050 110 (D17306) (2005).
- [3] H. Winnes, J. Moldanová, M. Anderson, E. Fridell. On-board measurements of particle emissions from marine engines using fuels with different sulphur content 30 (1) (2016) 45-54.

- [4] A.A. Reda, J. Schnelle-Kreis, J. Orasche, G. Abbaszade, J. Lintelmann, J.M. Arteaga-Salas, B. Stengel, R. Rabe, H. Harndorf, O. Sippula, T. Streibel, R. Zimmermann. Gas phase carbonyl compounds in ship emissions: Differences between diesel fuel and heavy fuel oil operation 112 (0) (2015) 370-380.
- [5] L. Mueller, G. Jakobi, H. Czech, B. Stengel, J. Orasche, J.M. Arteaga-Salas, E. Karg, M. Elsasser, O. Sippula, T. Streibel, J.G. Slowik, A.S.H. Prevot, J. Jokiniemi, R. Rabe, H. Harndorf, B. Michalke, J. Schnelle-Kreis, R. Zimmermann. Characteristics and temporal evolution of particulate emissions from a ship diesel engine 155 (2015) 204-217.
- [6] F. Di Natale and C. Carotenuto. Particulate matter in marine diesel engines exhausts: Emissions and control strategies 40 (2015) 166-191.
- [7] M. Anderson, K. Salo, Å.M. Hallquist, E. Fridell. Characterization of particles from a marine engine operating at low loads 101 (0) (2015) 65-71.
- [8] J. Blasco, V. Duran-Grados, M. Hampel, J. Moreno-Gutierrez. Towards an integrated environmental risk assessment of emissions from ships' propulsion systems 66 (2014) 44-7.
- [9] Z.D. Ristovski, B. Miljevic, N.C. Surawski, L. Morawska, K.M. Fong, F. Goh, I.A. Yang. Respiratory health effects of diesel particulate matter 17 (2) (2012) 201-212.
- [10] J.J. Corbett, J.J. Winebrake, E.H. Green, P. Kasibhatla, V. Eyring, A. Lauer. Mortality from Ship Emissions: A Global Assessment 41 (24) (2007) 8512-8518.
- [11] T. Chu-Van, T. Rainey, Z.D. Ristovski, A.M. Pourkhesalian, V. Garaniya, R. Abbassi, L. Yang, R.J. Brown, Emissions from a marine auxiliary diesel engine at berth using heavy fuel oil, Proceedings of the 10th AHMT Conference, Brisbane, Australia, 2016, p.81.
- [12] J. Moldanová, E. Fridell, O. Popovicheva, B. Demirdjian, V. Tishkova, A. Faccinotto, C. Focsa. Characterisation of particulate matter and gaseous emissions from a large ship diesel engine 43 (16) (2009) 2632-2641.
- [13] H. Agrawal, Q.G.J. Malloy, W.A. Welch, J. Wayne Miller, D.R. Cocker III. In-use gaseous and particulate matter emissions from a modern ocean going container vessel 42 (21) (2008) 5504-5510.
- [14] T. Chu-van
- [15] AVL List GmH, Boost Theory (v2014.1), AVL List GmbH: Graz, Austria, 2014.
- [16] L. Feng, J. Tian, W. Long, W. Gong, B. Du, D. Li, L. Chen. Decreasing NO_x of a low-speed two-stroke marine diesel engine by using in-cylinder emission control measures 9 (4) (2016).
- [17] F.V. Waldheim, M.J. Colaco and A.J.K. Leiroz, Numerical simulation of the performance of a marine engine using diesel and blends of marine diesel with ethanol, Proceedings of COBEM, Natal, Brazil, 2011.